



**HAL**  
open science

## Planum Temporale grey matter volume asymmetries in new-born monkeys (*Papio anubis*)

Yannick Becker, Romane Phelipon, Julien Sein, Lionel Velly, Luc Renaud, Adrien Meguerditchian

### ► To cite this version:

Yannick Becker, Romane Phelipon, Julien Sein, Lionel Velly, Luc Renaud, et al.. Planum Temporale grey matter volume asymmetries in new-born monkeys (*Papio anubis*). *Brain Structure and Function*, 2021, 10.1007/s00429-021-02278-9 . hal-03196979

**HAL Id: hal-03196979**

**<https://amu.hal.science/hal-03196979>**

Submitted on 13 Apr 2021

**HAL** is a multi-disciplinary open access archive for the deposit and dissemination of scientific research documents, whether they are published or not. The documents may come from teaching and research institutions in France or abroad, or from public or private research centers.

L'archive ouverte pluridisciplinaire **HAL**, est destinée au dépôt et à la diffusion de documents scientifiques de niveau recherche, publiés ou non, émanant des établissements d'enseignement et de recherche français ou étrangers, des laboratoires publics ou privés.

1 **Planum Temporale grey matter volume asymmetries in new-born monkeys (*Papio anubis*)**

2  
3 Yannick Becker<sup>1,2</sup>, Romane Phelipon<sup>1</sup>, Julien Sein<sup>2</sup>, Lionel Velly<sup>2</sup>, Luc Renaud<sup>2</sup> and Adrien  
4 Meguerditchian<sup>\*1,3</sup>

5 \*Corresponding Author: [adrien.meguerditchian@univ-amu.fr](mailto:adrien.meguerditchian@univ-amu.fr)

6  
7 <sup>1</sup> Laboratoire de Psychologie Cognitive, UMR 7290, Université Aix-Marseille / CNRS, 13331  
8 Marseille, France

9 <sup>2</sup> Institut des Neurosciences de la Timone, UMR 7289, Université Aix-Marseille / CNRS, 13005  
10 Marseille, France

11 <sup>3</sup> Station de Primatologie, CNRS, UPS846, 13790 Rousset, France

12  
13 **Abstract**

14 The Planum Temporale (*PT*) is one of the key hubs of the language network in the human brain. The  
15 gross asymmetry of this perisylvian region toward the left brain was considered as the most  
16 emblematic marker of hemispheric specialization of language processes in the brain. Interestingly, this  
17 neuroanatomical signature was documented also in newborn infants and preterms, suggesting the early  
18 brain's readiness for language acquisition. Nevertheless, this latter interpretation was questioned by a  
19 recent report in nonhuman primates of a potential similar signature in newborn baboons *Papio anubis*  
20 based on *PT* surface measures. Whether this "tip of the iceberg" *PT* asymmetry is actually reflecting  
21 asymmetry of its underlying grey matter volume remain unclear but critical to investigate potential  
22 continuities of cortical specialization with human infants. Here we report a population-level leftward  
23 asymmetry of the Planum Temporale grey matter volume in *in vivo* 34 newborn baboons *Papio*  
24 *anubis*, which showed intra-individual positive correlation with *PT* surface's asymmetry measures but  
25 also a more pronounced degree of leftward asymmetry at the population-level. This finding  
26 demonstrates that *PT* leftward structural asymmetry in this Old World monkey species is a robust  
27 phenomenon in early primate development, which clearly speaks for a continuity with early human  
28 brain specialization. Results also strengthen the hypothesis that early *PT* asymmetry might be not a  
29 human-specific marker for the pre-wired language-ready brain in infants.

30  
31 **Introduction**

32 The majority of language processes is asymmetric in the human brain, involving a  
33 specialization of the left hemisphere (Vigneau et al., 2006). The most emblematic marker of such a  
34 language cerebral organization is the gross asymmetry of the Planum Temporale (*PT*) toward the left  
35 hemisphere. This perisylvian region, which constitutes the floor of the Sylvian fissure, posterior to  
36 Heschl's gyrus and overlaps with Wernicke's area, is one of the key hubs of the language network in

37 the human brain. In fact, the left *PT* was significantly activated in a variety of language processing  
38 tasks in adults (Shapleske et al., 1999, Vigneau et al., 2006, Josse et al., 2006).

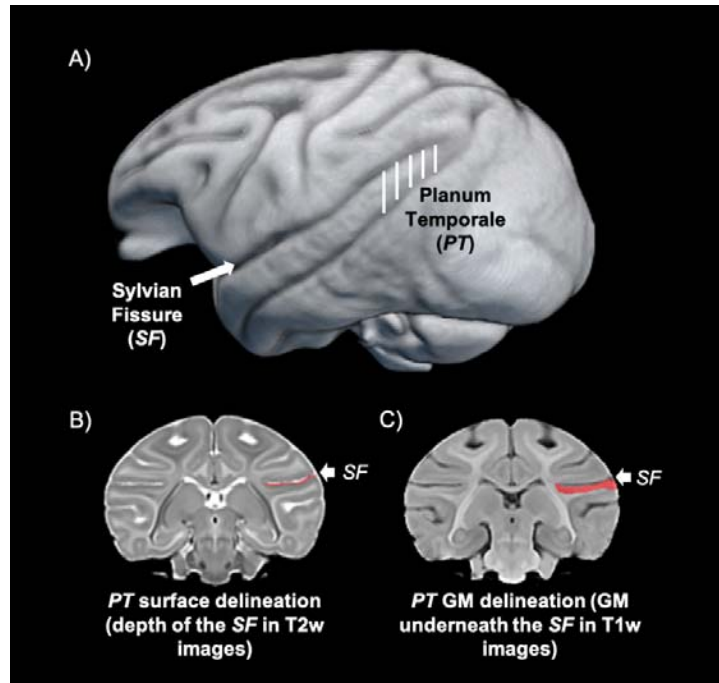
39 Since the first discovery that the *PT* was larger in the left hemisphere than the right in most  
40 adults (Geschwind and Levitsky, 1968), it remains unclear, whether this feature constitutes a good  
41 marker of language functional lateralization. While some studies reported no match between structural  
42 and functional asymmetry of this region (Keller, 2011; Greve, 2013), clinical studies found that  
43 atypical *PT* structural asymmetry were associated with multiple language deficits (Borovsky et al.,  
44 2007; Dronkers et al., 2004; Foundas et al., 2004; Wernicke, 1874). In addition, in a recent  
45 study, higher density of dendrites and axons in the *PT* were associated with faster neurophysiological  
46 processing of auditory speech (Ocklenburg et al., 2018). Moreover, in a second recent study,  
47 structural *PT* asymmetry was found associated with functional lateralization of an adjacent auditory  
48 area at the end of the Sylvian fissure during a language task (Tzourio-Mazoyer et al., 2018).

49 Interestingly, leftward *PT* asymmetry was detected early in the development at both the  
50 functional level in three-month-old infants in response to speech (Dehaene-Lambertz et al., 2002) and  
51 at the structural level in newborn and in preterms (Witelson and Pallie, 1973; Wada, 1975; Chi et al.,  
52 1977, Dubois et al., 2010; Hill et al., 2010; Glasel et al., 2011). Such early features of language brain  
53 lateralization suggest that the infant brain might be already pre-wired for language acquisition (e.g.  
54 Dehaene-Lambertz et al., 2002).

55 However, the human uniqueness of structural *PT* asymmetry was questioned by studies  
56 highlighting also a population-level leftward asymmetry by *PT* surface measures in chimpanzees  
57 (Gannon et al. 1998, Hopkins et al., 1998, Spocter et al. 2020) and in baboons (Marie et al. 2018). In  
58 this latter old world monkey species, *PT* leftward surface biases were found not only in adults but also  
59 recently in newborn baboons (Becker et al., 2021, see also Xia et al., 2019 for a study in macaques  
60 using cortical surface-based morphometry), suggesting it might reflect the asymmetry of its underlying  
61 grey matter volume and is thus not specific to human early brain development. In fact, *PT* surface  
62 area measures quantified the depth of the sylvian fissure's floor. It might be thus not excluded that the  
63 asymmetry of the sulcal surface area of this region might be an appropriate indicator of the asymmetry  
64 of the juxtaposing grey matter volume of the *PT*. This hypothesis is supported by few studies in adult  
65 chimpanzees which focused on *PT* grey matter volume asymmetry according to both ROI manual  
66 tracing (Hopkins and Nir, 2010; Lyn et al., 2011) and voxel-based morphometry (Hopkins et al.,  
67 2008), all showing consistent leftward asymmetry with *PT* surface measures.

68

69 In the present study, we further explore this hypothesis in 34 newborn baboons by quantifying the grey  
70 matter volume of the left and right *PT* from *in vivo* MRI brain scans (Becker et al., 2021). The aim of  
71 the follow-up study is thus to investigate early individual and population-level asymmetries of the *PT*  
72 grey matter volume in newborn nonhuman primates and their potential consistencies with *PT* surface  
73 asymmetries measures within the same cohort of subjects used in Becker et al.'s study (2021).



74  
75 **Figure 1.** (A) 3D reconstruction of a newborn baboon brain with the *PT* region highlighted by the  
76 white lines (B) Coronal slice of the same subject with the delineation of the Sylvian Fissure's floor (in  
77 red), used for *PT* surface measures (C) Coronal slice of the same subject with the delineation of the  
78 grey matter (in red) underneath the Sylvian Fissure, used for *PT* volume measures.

79

## 80 **Materials and Methods**

### 81 Subjects

82 Subjects ranged from 4 to 165 days of age (Mean: 32.63; SD: 6.13) and included 21 males and 14  
83 females. (see table in supplementary methods with subjects' details)

84 All monkeys are housed in social groups at the Station de Primatologie CNRS (UPS 846, Rousset,  
85 France) and have free access to outdoor areas connected to indoor areas. All subjects are born in  
86 captivity from 1 (F1) or 2 generations (F2). Wooden and metallic structures enrich the enclosures.  
87 Feeding times are held four times a day with seeds, monkey pellets and fresh fruits and vegetables.  
88 Water is available ad libitum.

89

90

91 *MRI Image acquisition*

92 Structural magnetic resonance images (MRI) were collected from a sample of 35 baboons (September  
93 2017 to March 2020). Animals were minimally anesthetized by a veterinarian; and vital functions  
94 were monitored during the scans. High-resolution structural T1-weighted brain images were obtained  
95 with MPRAGE sequences (0.4 mm isotropic, TR = 2500ms, TE = 3.01ms) with the subject in the  
96 supine position on a Siemens 3T Magnetom Prisma scanner and using two 11cm receive-only loop  
97 coils (for more detailed procedure: Becker et al., 2021). At the end of the MRI session, when fully  
98 awaked from anaesthesia, baboons were carefully put back with their mother and then transported for  
99 immediate (or delayed) reintroduction into their social groups under staff monitoring.

100

101 *Preprocessing of Anatomical MRI*

102 Anatomical T1w images were noise corrected with the spatially adaptive nonlocal means denoising  
103 filter (Manjón et al., 2010) implemented in Cat12 toolbox (<http://www.neuro.uni-jena.de/cat/>)  
104 included in SPM12 (<http://www.fil.ion.ucl.ac.uk/>), which runs on MATLAB (R2014a). Next, each  
105 image was manually oriented using ITK-Snap 3.6 according anterior and posterior commissures plane  
106 and the interhemispheric fissure plane.

107

108 *Manual Delineation of the Planum Temporale's grey matter volume*

109 Manual delineation was conducted with "ANALYZE 11.0 (AnalyzeDirect)" software and following  
110 the delimitation instructions established in previous *PT* studies in nonhuman primates using MRI (e.g.,  
111 Hopkins and Nir, 2010; Lyn et al., 2011; Meguerditchian et al., 2012; Marie et al., 2018; Becker et al.,  
112 2021). The delineation of the posterior edge of the *PT* is defined by the most caudal section showing  
113 the Sylvian fissure. In humans, the anterior edge of the *PT* is delimited by the Heschl gyrus, however,  
114 in baboons the Heschl gyrus is not clearly detectable, therefore to delineate the anterior edge of the *PT*  
115 here, the most anterior cut including the Sylvius Fissure was used when the insula closes completely  
116 (when the insula fissure disappears completely posteriorly). For each slice, manual tracing was  
117 conducted from the medial most point of the Sylvius Fissure, to the most lateral point, following the  
118 most ventral edge of the fissure. Next, the raters followed the grey matter to its most inferior edge of  
119 the grey/white matter boundary. When ambiguous, the imaginary prolongation of the Sylvian Fissure  
120 was used to differentiate between the grey matter of interest and the more dorsal gyrus. This step is  
121 repeated on the next cut, advancing posteriorly, until the Sylvius Fissure disappears. If the fissure  
122 forked in an ascending or descending direction, it was preferable to follow the descending one. This  
123 manual tracing was done on the coronal plane and not sagittal, as it gives the best assessment of the  
124 total depth of the Sylvius pit, which is the "ground" of the *PT*. The manual delimitation was carried  
125 out via a graphic tablet (WACOM cintiq 13HD). Out of the 256 slices included in the MRI images, the  
126 *PT* appeared in about 20 slices (Supplementary Figure 1)

127 For each subject, an Asymmetry Quotient (AQ) of the left (L) and the right (R) grey matter volume  
128 was computed  $AQ = (R - L) / [(R + L) \times 0.5]$  with the sign indicating the direction of asymmetry  
129 (negative: left side, positive: right side) and the value, the strength of asymmetry. Further, as reported  
130 by Hopkins and Nir (2010) for humans and great apes, the AQ was also used to classify the subjects as  
131 left-hemispheric biased ( $AQ \leq -0.025$ ), right biased ( $AQ \geq 0.025$ ), or non-significantly biased “ambi”  
132 ( $-0.025 < AQ < 0.025$ ).

133 To reduce potential observer-dependent manual tracing biases, all the *PTs* grey matter volume were  
134 traced by a rater different from the one who traced the *PT* surface in Becker et al. (2021). The rater of  
135 the present study was blind to the *PT* surface’s tracing, data and results of Becker et al. (2021).  
136 Statistics were conducted with R 3.6.1 (R Core Team (2017). R: A language and environment for  
137 statistical computing. R Foundation for Statistical Computing, Vienna, Austria. URL [https://www.R-](https://www.R-project.org/)  
138 [project.org/.](https://www.R-project.org/))

139

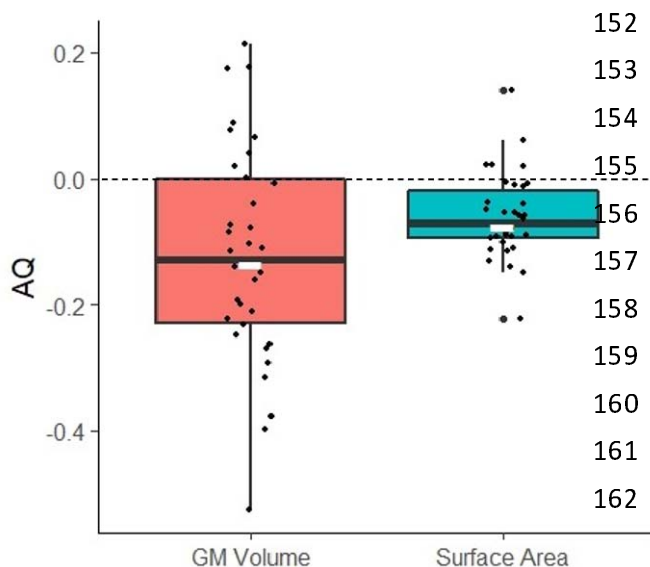
## 140 Results

### 141 *PT Grey matter volume measures*

142 We found a significant leftward asymmetry of the *PT* grey matter volume at a group-level in 34  
143 newborn baboons according to a one sample t-test in the 34 subjects AQ scores (see Figure 2), *Mean*  
144  $AQ = -0.121$ ,  $0.169$  SD;  $t(33) = -4.2$ ,  $p < 0.0001$ . Categorization of individual AQ showed also a  
145 majority of leftward *PT*-biased individuals: 24 baboons exhibited a leftward hemispheric *PT* bias  
146 (70.6%) whereas 7 exhibited a rightward *PT* bias (19.6%) and 3 no *PT* bias (8.8%). The number of  
147 leftward *PT*-biased individuals was significantly greater than the number of rightward *PT*-biased  
148 according to chi-square test ( $\chi^2 = 21.94$ ,  $p < 0.0001$ ).

149 Multiple linear regression analyses showed that the right *PT* volume ( $p < 0.001$ ) and the left *PT*  
150 volume ( $p < 0.001$ ) predict *PT* asymmetry strength, but not the subject’s sex, age nor brain volume.

151



152 **Figure 2.** Distribution of Asymmetry  
153 Quotients (AQ) for Grey Matter (GM)  
154 volume measures in red and Surface area  
155 measures in blue for the same subjects. AQ  
156 values inferior to 0 indicate leftward  
157 lateralization, AQ values superior to 0  
158 indicate rightward lateralization. Note the  
159 leftward lateralization for both measure  
160 types. Note also larger distribution, ie.  
161 higher AQ values for the grey matter  
162 volume measures.

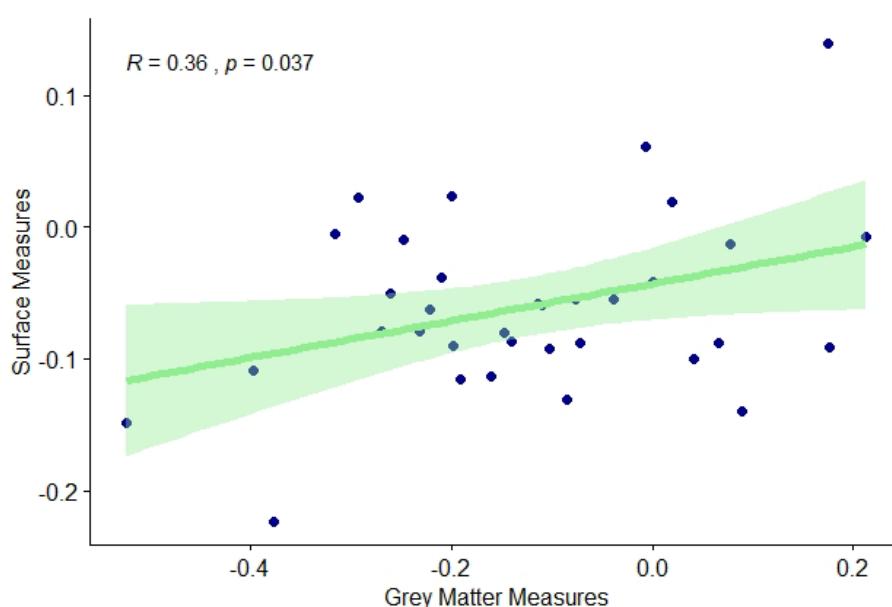
163

164 Correspondence between PT Surface and PT Grey Matter measures

165 Within the 34 individuals for whom data of *PT* surface and *PT* grey matter volume measures were  
166 independently traced by two different raters blind to the results of each other, a significant positive  
167 intra-individual correlation of AQ scores was found between *PT* surface and *PT* grey matter volume.  
168  $r(34) = 0.36, p < 0.037$ .

169 In comparison to previous surface *PT* measures (Becker et al., 2021), 22 were consistent in  
170 hemispheric lateralization classification (i.e., 20 leftward, 1 rightward and 1 ambi) and 4 subjects  
171 switched direction of hemispheric *PT* bias (i.e., from leftward bias for *PT* surface to rightward bias for  
172 *PT* grey matter volume). Among the remaining 8 subjects, 6 which previously showed no significant  
173 bias (i.e. “ambi”) for the *PT* surface were found significantly lateralized for the *PT* grey matter volume  
174 and 2 which were previously classified as significantly lateralized for the *PT* surface were classified as  
175 “ambi” for the *PT* grey matter volume.

176



177 **Figure 3.** Pearson correlation between *PT* Surface and Grey matter volume measures.

178

179

180 **Discussion:**

181 We find for the first time both individual and leftward population-level grey matter volume  
182 asymmetries of the Planum Temporale not only in Old World monkeys but also in a newborn non-  
183 human primate. These results showed intra-individual positive correlation with previous published *PT*  
184 surface measures on the same subjects as well as consistent leftward *PT* asymmetry (Becker et al.,  
185 2021) and suggesting *PT* surface measures may therefore reflect its underlying grey matter volume.

186 The distributions of individual *PT* hemispheric preferences (left, right or ambi) are quite

187 similar between volumetric grey matter and surfacic measures, especially for the left lateralized  
188 subjects, although some inconsistency was noticed at the individual level in a minority of subjects. It  
189 remains unclear whether those variations are due to interrater-dependent variability in the measures,  
190 which leads few subjects to switch categories or to the possibility that *PT* surface measures are not  
191 entirely perfect “tip of the iceberg” predictors of the *PT* grey matter volume, especially for the subjects  
192 initially classified as ambiguously biased for *PT* surface. In fact, almost all of those latter “ambi”  
193 newborns (6 out of 7) were found to be significantly lateralized for *PT* grey volume. In addition, AQ  
194 values were overall higher in grey matter measures (AQ -0.121 12.1%) compared to surface measures  
195 (AQ -0.073 7.3%). A similar effect was found in Hopkins and Nir’s paper (2010), which showed a  
196 4.96% larger left hemisphere when measuring its surface and 6.63% larger hemisphere when  
197 measuring its grey matter. Therefore, measures of grey matter volume may be more likely to capture  
198 interindividual differences of the *PT* asymmetry, whereas the surface measures may only scratch the  
199 top of the *PT* iceberg.

200 Interestingly, in a previous study in chimpanzees, Hopkins and Nir (2010) noted that leftward  
201 *PT* grey matter volume asymmetry constituted a better marker for the chimpanzee’s right-hand  
202 preference in communicative pointing gestures than *PT* surface (but see Meguerditchian et al., 2012).  
203 This latter study suggested the hypothesis that asymmetry of *PT* grey matter volume might be  
204 associated to functional asymmetry related to properties of gestural communication in apes, which  
205 have been found to share common features with human language such as intentionality, flexibility or  
206 referential properties (i.e., Liebal et al., 2013). Communicative manual gestures in baboons were also  
207 described in the literature (e.g., Molesti et al., 2020) as well as their chimpanzees-like manual  
208 lateralization patterns (Meguerditchian et al. 2013). Follow-up behavioral observations on gestural  
209 lateralization for communication in our sample of growing baboons will advance this question, once  
210 the focal subjects develop their full gestural repertoire. Specifically, taking advantage of the stronger  
211 *PT* asymmetries described in the present study for grey matter volume in comparison to surface  
212 measures, we could further investigate whether those early brain asymmetries might predict the  
213 gestural lateralization’s emergence in later development.

214 In conclusion, the present finding in nonhuman infants provides additional support to the hypothesis of  
215 a continuity between nonhuman and human primates concerning early leftward structural *PT*  
216 asymmetry in brain development. Early *PT* asymmetry might be thus not a human-specific marker for  
217 the pre-wired language-ready brain in infants. Nevertheless, it might be not excluded that this common  
218 anatomical signature is related to an ancient shared cognitive process at the heart of language  
219 evolution.

220

## 221 **Acknowledgments**

222 We are very grateful to the vets Romain Lacoste and Marie Dumasy as well as the anesthetist Laura  
223 Laura Giacomino for supervising the first health and anesthesia monitoring, Emilie Rapha for great



224 assistance and animal care, Frederic Charlin, as well as the care staff of the Station de Primatologie,  
225 such as Valérie Moulin, Brigitte Rimbaud, Richard Francioly, the vets Pascaline Boitelle, Alexia  
226 Cermolacce & Janneke Verschoor, the behavioral manager Pau Molina, the engineers of the MRI  
227 center, Bruno Nazarian and Jean-Luc Anton for coordinating the MRI sessions.

228

### 229 **Funding**

230 The project has received funding from the European Research Council under the European Union's  
231 Horizon 2020 research and innovation program grant agreement No [716931](#) - GESTIMAGE - ERC-  
232 2016-STG (P.I. Adrien Meguerditchian), from the French “Agence Nationale de le Recherche” ANR-  
233 16-CONV-0002 (ILCB) and the Excellence Initiative of Aix-Marseille University (A\*MIDEX). This  
234 MRI acquisitions were done at the Center IRM-INT (UMR 7289, AMU-CNRS), platform member of  
235 France Life Imaging network (grant ANR-11-INBS-0006).

236

### 237 **Conflicts of interest/Competing interests**

238 Not applicable

239

### 240 **Availability of data and material**

241 See supplementary material

242

### 243 **Code availability**

244 Not applicable

### 245 **Authors' contributions**

246 Y.B and A.M prepared the paper and the revision. R.P. performed the tracing and analyses. J.S.  
247 parametrized the MRI sequences and optimized the MRI acquisition setup. L.V. and L.R. designed  
248 and performed respectively the specific procedures of welfare, anesthesia, monitoring and preparation  
249 of baboons in the MRI machine. A.M. designed and supervised the study and MRI acquisitions.

250

### 251 **Ethics approval**

252 All animal procedures were approved by the “C2EA -71 Ethical Committee of neurosciences” (INT  
253 Marseille) under the number APAFIS#13553-201802151547729 v4 and has been conducted at the  
254 Station de Primatologie under the number agreement C130877 for conducting experiments on  
255 vertebrate animals (Rousset-Sur-Arc, France). All methods were performed in accordance with the  
256 relevant French law, CNRS guidelines and the European Union regulations (Directive 2010/63/EU).

257

258

259

260

261

262

263 **References**

- 264 Becker Y, Sein J, Velly L, et al (2021) Early Left-Planum Temporale Asymmetry in Newborn  
265 Monkeys (*Papio anubis*): A longitudinal structural MRI study at two stages of development.  
266 *NeuroImage* 117575. <https://doi.org/10.1016/j.neuroimage.2020.117575>
- 267 Borovsky A, Saygin AP, Bates E, Dronkers N (2007) Lesion correlates of conversational speech  
268 production deficits. *Neuropsychologia* 45:2525–2533.  
269 <https://doi.org/10.1016/j.neuropsychologia.2007.03.023>
- 270 Chi JG, Dooling EC, Gilles FH (1977) Left-Right Asymmetries of the Temporal Speech Areas of the  
271 Human Fetus. *Archives of Neurology* 34:346–348.  
272 <https://doi.org/10.1001/archneur.1977.00500180040008>
- 273 Dehaene-Lambertz G, Dehaene S, Hertz-Pannier L (2002) Functional Neuroimaging of Speech  
274 Perception in Infants. *Science* 298:2013–2015. <https://doi.org/10.1126/science.1077066>
- 275 Dronkers NF, Wilkins DP, Van Valin RD, et al (2004) Lesion analysis of the brain areas involved in  
276 language comprehension. *Cognition* 92:145–177. <https://doi.org/10.1016/j.cognition.2003.11.002>
- 277 Dubois J, Benders M, Lazeyras F, et al (2010) Structural asymmetries of perisylvian regions in the  
278 preterm newborn. *NeuroImage* 52:32–42. <https://doi.org/10.1016/j.neuroimage.2010.03.054>
- 279 Foundas AL, Bollich AM, Feldman J, et al (2004) Aberrant auditory processing and atypical planum  
280 temporale in developmental stuttering. *Neurology* 63:1640–1646.  
281 <https://doi.org/10.1212/01.WNL.0000142993.33158.2A>
- 282 Gannon PJ, Holloway RL, Broadfield DC, Braun AR (1998) Asymmetry of Chimpanzee Planum  
283 Temporale: Humanlike Pattern of Wernicke’s Brain Language Area Homolog. *Science* 279:220–  
284 222. <https://doi.org/10.1126/science.279.5348.220>
- 285 Geschwind N, Levitsky W (1968) Human Brain: Left-Right Asymmetries in Temporal Speech  
286 Region. *Science* 161:186–187. <https://doi.org/10.1126/science.161.3837.186>
- 287 Glasel H, Leroy F, Dubois J, et al (2011) A robust cerebral asymmetry in the infant brain: The  
288 rightward superior temporal sulcus. *NeuroImage* 58:716–723.  
289 <https://doi.org/10.1016/j.neuroimage.2011.06.016>
- 290 Greve DN, Van der Haegen L, Cai Q, et al (2013) A surface-based analysis of language lateralization  
291 and cortical asymmetry. *J Cogn Neurosci* 25:1477–1492. [https://doi.org/10.1162/jocn\\_a\\_00405](https://doi.org/10.1162/jocn_a_00405)
- 292 Hill J, Inder T, Neil J, et al (2010) Similar patterns of cortical expansion during human development  
293 and evolution. *Proceedings of the National Academy of Sciences* 107:13135–13140.  
294 <https://doi.org/10.1073/pnas.1001229107>
- 295 Hopkins WD, Marino L, Rilling JK, MacGregor LA (1998) Planum temporale asymmetries in great  
296 apes as revealed by magnetic resonance imaging (MRI). *NeuroReport* 9:2913–2918

- 297 Hopkins WD, Nir TM (2010) Planum temporale surface area and grey matter asymmetries in  
298 chimpanzees (*Pan troglodytes*): The effect of handedness and comparison with findings in  
299 humans. *Behavioural Brain Research* 208:436–443. <https://doi.org/10.1016/j.bbr.2009.12.012>
- 300 Hopkins, W. D., Tagliabata, J. P., Meguerditchian, A., Nir, T., Schenker, N. M., & Sherwood, C. C.  
301 (2008). Gray matter asymmetries in chimpanzees as revealed by voxel-based morphology.  
302 *Neuroimage*, 42, 491-497.
- 303 Josse G, Hervé P-Y, Crivello F, et al (2006) Hemispheric specialization for language: Brain volume  
304 matters. *Brain Research* 1068:184–193. <https://doi.org/10.1016/j.brainres.2005.11.037>
- 305 Keller SS, Roberts N, García-Fiñana M, et al (2010) Can the Language-dominant Hemisphere Be  
306 Predicted by Brain Anatomy? *Journal of Cognitive Neuroscience* 23:2013–2029.  
307 <https://doi.org/10.1162/jocn.2010.21563>
- 308 Liebal, K., Waller, B. M., Burrows, A. M., & Slocombe, K. E. (2013). *Primate communication: A*  
309 *multimodal approach*. Cambridge: Cambridge University Press.
- 310 Lyn, H., Pierre, P., Bennett, A. J., Fears, S., Woods, R., & Hopkins, W. D. (2011). Planum temporale  
311 grey matter asymmetries in chimpanzees (*Pan troglodytes*), vervet (*Chlorocebus aethiops*  
312 *sabaeus*), rhesus (*Macaca mulatta*) and bonnet (*Macaca radiata*) monkeys. *Neuropsychologia*, 49,  
313 2004-2012.
- 314 Manjón JV, Coupé P, Martí-Bonmatí L, et al (2010) Adaptive non-local means denoising of MR  
315 images with spatially varying noise levels. *Journal of Magnetic Resonance Imaging* 31:192–203.  
316 <https://doi.org/10.1002/jmri.22003>
- 317 Marie D, Roth M, Lacoste R, et al (2018) Left Brain Asymmetry of the Planum Temporale in a  
318 Nonhominid Primate: Redefining the Origin of Brain Specialization for Language. *Cereb Cortex*  
319 28:1808–1815. <https://doi.org/10.1093/cercor/bhx096>
- 320 Meguerditchian A, Gardner MJ, Schapiro SJ, Hopkins WD (2012) The sound of one-hand clapping:  
321 handedness and perisylvian neural correlates of a communicative gesture in chimpanzees. *Proc*  
322 *Biol Sci* 279:1959–1966. <https://doi.org/10.1098/rspb.2011.2485>
- 323 Meguerditchian A, Vauclair J, Hopkins WD (2013) On the origins of human handedness and  
324 language: A comparative review of hand preferences for bimanual coordinated actions and  
325 gestural communication in nonhuman primates. *Developmental Psychobiology* 55:637–650.  
326 <https://doi.org/10.1002/dev.21150>
- 327 Molesti, S., Meguerditchian, A., & Bourjade, M. (2020). Gestural communication in olive baboons  
328 (*Papio anubis*): repertoire and intentionality. *Animal Cognition*, 23, 19–40.
- 329 Ocklenburg S, Friedrich P, Fraenz C, et al (2018) Neurite architecture of the planum temporale  
330 predicts neurophysiological processing of auditory speech. *Science Advances* 4:eaar6830.  
331 <https://doi.org/10.1126/sciadv.aar6830>

- 332 Shapleske J, Rossell SL, Woodruff PWR, David AS (1999) The planum temporale: a systematic,  
333 quantitative review of its structural, functional and clinical significance. *Brain Research Reviews*  
334 29:26–49. [https://doi.org/10.1016/S0165-0173\(98\)00047-2](https://doi.org/10.1016/S0165-0173(98)00047-2)
- 335 Spocter MA, Sherwood CC, Schapiro SJ, Hopkins WD (2020) Reproducibility of leftward planum  
336 temporale asymmetries in two genetically isolated populations of chimpanzees (*Pan troglodytes*).  
337 *Proc R Soc B* 287:20201320. <https://doi.org/10.1098/rspb.2020.1320>
- 338 Tzourio-Mazoyer N, Crivello F, Mazoyer B (2018) Is the planum temporale surface area a marker of  
339 hemispheric or regional language lateralization? *Brain Struct Funct* 223:1217–1228.  
340 <https://doi.org/10.1007/s00429-017-1551-7>
- 341 Vigneau M, Beaucousin V, Hervé PY, et al (2006) Meta-analyzing left hemisphere language areas:  
342 Phonology, semantics, and sentence processing. *NeuroImage* 30:1414–1432.  
343 <https://doi.org/10.1016/j.neuroimage.2005.11.002>
- 344 Wada JA (1975) Cerebral Hemispheric Asymmetry in Humans: Cortical Speech Zones in 100 Adult  
345 and 100 Infant Brains. *Archives of Neurology* 32:239.  
346 <https://doi.org/10.1001/archneur.1975.00490460055007>
- 347 Wernicke C (1874) *Der aphasische Symptomencomplex: Eine psychologische Studie auf*  
348 *anatomischer Basis*. Cohn.
- 349 Witelson SF, Pallie W (1973) Left Hemisphere Specialization for Language in the Newborn:  
350 neuroanatomical Evidence of Asymmetry. *Brain* 96:641–646.  
351 <https://doi.org/10.1093/brain/96.3.641>
- 352 Xia, J., Wang, F., Wu, Z., Wang, L., Zhang, C., Shen, D., Li, G., 2019. Mapping hemispheric  
353 asymmetries of the macaque cerebral cortex during early brain development. *Hum. Brain Map.*  
354 doi: 10.1002/hbm.24789.